Monthly Notices of the ROYAL ASTRONOMICAL SOCIETY

MNRAS **527,** 1368–1380 (2024) https://doi.org/10.1093/mnras/stad3264
Advance Access publication 2023 October 25

Properties of isolated galaxies in the Digital Survey Isolated Galaxies (DSIG) catalogue within a redshift range ($0.005 < z < 0.080$)

Marcelina K. Kinyumu,[1]★ Naftali Kimani,[1]★ Raphael Nyenge[1] and Willice Obonyo[2]

[1]*Department of Physics, Kenyatta University, PO Box 43844, 00100 Nairobi, Kenya*
[2]*Department of Astronomy and Space Science, Technical University of Kenya, PO Box 52428, 00200 Nairobi, Kenya*

Accepted 2023 October 19. Received 2023 October 16; in original form 2023 August 10

ABSTRACT

Evolution of galaxies is known to be influenced by a number of factors such as the environment that hosts the galaxy as well as the galaxies intrinsic properties. The environmental effects on galaxy properties have not been fully quantified. In our study, we analysed a sample of isolated galaxies within $0.005 < z < 0.080$ from Sloan Digital Sky Survey data release 16, as part of a Digital Survey Isolated Galaxies catalogue. The aim was to investigate intrinsic physical properties of singly isolated galaxies in low-density environment. We investigated the galaxies morphology, colour, luminosity, stellar masses, and star formation rates (SFRs). A concentration index, C_r, of 2.65 separates our isolated sample into early and late types, with the late-types (spiral galaxies) dominating the isolated sample at 68 per cent as confirmed from the visually classified sample obtained from Galaxy Zoo. Our isolated ellipticals are redder, massive, and more luminous, while the isolated spirals are blue, less massive, and less luminous. Both the isolated spirals and ellipticals have steeper colour relations indicating a fast transition to the red sequence. In the colour–colour analysis, most ellipticals were quiescent with the majority of spirals being star forming. 5 per cent of the isolated ellipticals have recently quenched their star formation and are transiting to the red sequence. The isolated spirals experiences higher star-forming activities, with a small fraction of passively evolving high-mass isolated spirals. Similarly, isolated ellipticals exhibit low SFRs indicating passive evolution, with a fraction being actively star forming.

Key words: methods: statistical – galaxies: evolution – galaxies: fundamental parameters – galaxies: star formation.

1 INTRODUCTION

Understanding the process of formation and evolution of galaxies continues to be an active topic of discussion but quite complex. Its complex nature can be attributed to processes such as star formation, galaxy environment, perturbation effects, and galaxy mergers (Kauffmann et al. 2002; Niemi et al. 2010; Lacerna et al. 2014). Other influential properties include, density of protogalactic clouds and galaxy masses (Fernández Lorenzo et al. 2013).

The current galaxy formation model, the lambda-cold dark matter model, predicts that galaxies in their initial stages form as late types or disc-like. This is a result of the cooling of gas with an angular momentum greater than zero, in virialized dark matter haloes. In the following hierarchical evolution, a variety of mechanisms transform late-type galaxies into early type leading to a transformation in the morphology or quenching of star formation or both (Van Den Bosch et al. 2008).

Some physical processes contributing to the transformation of late- to early-type galaxies have been suggested, for example, the late-type galaxies being transformed to early type during a major merger (Hopkins et al. 2006). Physical processes predicted the quenching of star formation by either removing the cold gas, which is essential in fuelling the production of new stars, heating, or cutting off its supply. In satellite galaxies, which are companion galaxies orbiting within the gravitational potential of their host galaxies, the mechanisms quenching star formation are strangulation and ram pressure. The morphological transformation of galaxies from discs to spheroid can be attributed to harassment and tidal stripping (Van Den Bosch et al. 2008). Different morphological classes observed currently are known to have a significant dependence on the environment in which the galaxies are located (Vollmer 2013; Argudo-Fernández et al. 2015).

There is an observational agreement, up to a redshift of $z \sim 1$, where early types as compared to spirals and irregulars, are massive, luminous, red, and old (Bell et al. 2003b; Bolzonella et al. 2010; Pozzetti et al. 2010). Early-type galaxies which are supported by their rotation are approximately 60 per cent with no significant change from a redshift of approximately $z \sim 0$ to ~ 1 according to Van Der Wel & Van Der Marel (2008). They are preferentially found in dense, cluster-like regions, while late types mainly reside in low-density environments (Gabor et al. 2010). Getting insight on processes governing the transformation of galaxy morphological structure and/or star formation quenching process is essential in the theory of galaxy formation and evolution.

The study of isolated galaxies is significant in understanding the intrinsic mechanisms and processes affecting galaxy evolution. It is important to have a galaxy sample where the effect of both the local and large-scale environments are minimized and quantified. Analysing the properties of isolated galaxies, gives insight on the

★ E-mail: marcelinerkinyumu@gmail.com (MK); kimani.naftali@ku.ac.ke (NK)

influence, and environmental dependence, of galaxy properties, in galaxy evolution. A number of galaxy properties that can be investigated include; morphology, colour, luminousity, stellar masses, and star formation rates (SFRs).

According to Verdes-Montenegro et al. (2005), isolated galaxies are assumed to have escaped a significant influence from their neighbours, for a crossing time of approximately 3 Gyr. The observed properties of such galaxies therefore are most likely depended on the galaxies initial formation conditions, together with other evolution processes (Coziol et al. 2011; Fernández Lorenzo et al. 2013). Most isolated galaxies are found surrounding filaments, walls, and clusters, and are generally taken to be different form the population of galaxies in void environments (Argudo-Fernández et al. 2015).

In this work, we present a description of the sample and data used in Section 2. We highlight the results of our analysis in Section 3, and present a detailed discussion in Section 4. Finally, we provide a summarised conclusion of the main results and findings in Section 5. Throughout the study, we assumed the cosmological parameters $\Omega_{\Lambda 0} = 0.7$, $\Omega_{m0} = 0.3$, and $H_0 = 70\,\mathrm{km\,s^{-1}\,Mpc^{-1}}$.

2 ARCHIVAL DATA AND SAMPLE SELECTION

2.1 The isolated galaxy sample

Studying isolated galaxies is fundamental in understanding the role played by environment in the galaxies formation and evolution process. In our analysis, we used a sample of singly isolated galaxies compiled by Argudo-Fernández et al. (2015), based on the Tenth Data Release of the Sloan Digital Sky Survey (SDSS-DR10, Ahn et al. 2014). The sample was selected following a 3D isolation criterion that includes a defined line of sight velocity, a specified field radius, and a final visual inspection of all the selected galaxies for inclusion in the final catalogue.

The primary sample was composed of galaxies from the main spectroscopic sample (Strauss et al. 2002) with r-band model magnitudes in the range $11 \leq m_r \leq 15.7$, which is sufficient to develop a homogeneous isolation definition (for a neighbour sample) 2 mag fainter than the primary, since the redshift completeness of the SDSS is $m_{r,\,\mathrm{Petrosian}} < 17.77$ mag. The galaxy sample was selected to have the redshift range within $0.005 \leq z \leq 0.080$. Galaxies with redshift lower than 0.005 were discarded to avoid nearby sources for which isolation cannot be estimated well (Verley et al. 2007) and larger errors from photometry for very extended galaxies. Galaxies with redshift above 0.080 were also discarded to facilitate studies based on visual morphological classifications.

The sample utilised is part of a Digital Survey Isolated Galaxies catalogue, DSIG. The catalogue of singly isolated galaxies, (which we will refer to as SIG) is composed of 3702 galaxies with no neighbours within a velocity difference of $\Delta v \leq 500\,\mathrm{km\,s^{-1}}$ and a field radius of 1 Mpc. All the systems in the catalogue were visually inspected. While the catalogue is publicly available, a more description can be found in Argudo-Fernández et al. (2015), and references therein.

2.2 Galaxies in the Coma cluster

The Coma cluster (Abell 1656) is a nearby rich cluster (at a distance of 100 Mpc and velocity dispersion of $1000\,\mathrm{km\,s^{-1}}$), and one of the most well-studied galaxy clusters (Biviano et al. 1995; Healy et al. 2021). As a dense cluster, it serves as an excellent control sample in our analysis. We use a catalogue of 850 spectroscopically confirmed members of the Coma cluster within a 2 deg radius of the cluster centre, from the Westerbork Coma Survey (WCS), which is a compiled redshift catalogue of the Coma cluster. The catalogue of unique sources, associated with the Coma cluster, was constructed considering sources with velocities $3000 < cz < 10\,500\,\mathrm{km\,s^{-1}}$. The WCS catalogue is described in Healy et al. (2021).

2.3 The Galaxy Zoo catalogue

Classification of galaxies into the two main morphological types, the late-type (spirals) and early types which include ellipticals and lenticulars (S0), is essential when studying properties of galaxies (Shimasaku et al. 2001). For our analysis, we obtained visual morphological classifications from the Galaxy Zoo catalogue, which contains visual classifications for main galaxies available in the SDSS-DR8.

The catalogue contains raw votes, weighted elliptical (E) and combined spiral (CS) category votes, and flags for the inclusion of the galaxies in a clean, debiased catalogue. The debias vote being where bias correction has been applied to votes and the clean fraction is defined as having a debiased vote of greater than 0.8 for the respective categories. However, debiased calculations are available for spectroscopically observed galaxies. We separated our sample into the elliptical and spiral categories. In the classification, we used the majority debias vote fraction from the E and CS categories to assign the galaxies to the category with the larger vote fraction, respectively. A detailed description on the classifications and corrections of the zoo mophologies is presented by Lintott et al. (2008, 2011).

2.4 Photometry and spectroscopy

In this study, we used both photometric and spectroscopic data from SDSS-DR 16 (the Sloan Digital Sky Survey, data release sixteen, Ahumada et al. 2020). SDSS is a Northern Sky survey with photometric data in u, g, r, i, and z filters (Fukugita et al. 1996; Gunn et al. 1998). The SDSS-DR16 survey has performed photometric and spectroscopic observations using a 3 arcsec diameter fibres giving an acceptable sample complete to $r < 17.77$ (Blanton et al. 2003). The spectral range covered is between 3800 ß and 9200 ß. For the galaxies, we retrieved SDSS model magnitudes (model Mag) for filters u, g, r, i, z, and optical spectra in CasJobs query.

3 PROPERTIES OF ISOLATED GALAXIES

3.1 Morphological classifications

Classification of galaxies into different morphological types is essential when studying galaxy properties (Shimasaku et al. 2001). Galaxies have traditionally been morphologically classified by eye (De Vaucouleurs et al. 1991; Fukugita et al. 2007). None the less, visually classifying galaxies is labour intensive and very time consuming. When galaxy samples are large, automated classification schemes are often preferred. A widely used automated classifying alternative is the central concentration selection index, C_r, a parameter that can reliably differentiate late types (Sa, Sb, Sc, and Irr) and early types (E and SO) (Shimasaku et al. 2001). In the next section, we investigate the use of concentration index as a morphological classification tool in isolated galaxies.

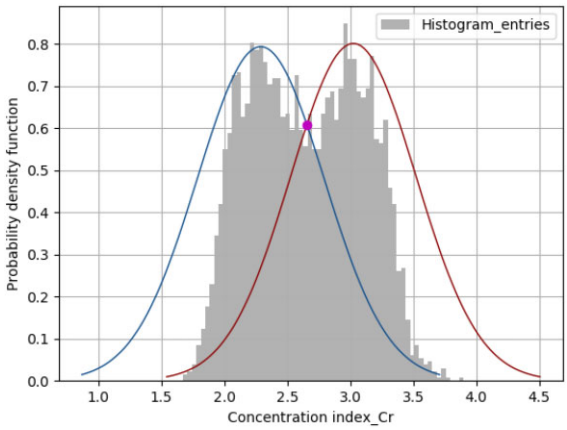

Figure 1. A histogram plot with concentration index and a double Gaussian fit for our sample of singly isolated galaxies. The two curves represent the Gaussian fit. A point at the intersection of the two lines is the concentration index separation value of 2.65 for the two distributions. The area of overlap gives an estimate of the classification contamination of the sample, where the classifications are ambiguous.

Table 1. The isolated galaxy sample classification results with the concentration index (C_r of 2.65).

	No. of galaxies (C_r)	Percentage	Total contamination (per cent)
Late type	1856	50.18	
Early type	1843	49.82	
Sum	3699		46.20

3.1.1 Concentration index

For galaxies in SDSS, the concentration index C_r, is given by the ratio R90/R50, with R90 being the radii enclosing 90 per cent, while R50 enclosing 50 per cent of the *r* Petrosian flux (Shimasaku et al. 2001; Strateva et al. 2001; Nakamura et al. 2003). The Petrosian flux is the flux within two times the Petrosian radius, the circular radius where 20 per cent of the enclosed mean surface brightness is the local surface brightness $\mu(r)$ (Blanton et al. 2003). To classify our sample, we retrieved SDSS petroR90 and petroR50 *r*-band magnitudes from the SDSS-DR16 data base.

In separating our sample of isolated galaxies into early and late types with the concentration index, we first plotted a histogram distribution as in Fig. 1. We fitted two Gaussians to the distribution and taking the point of interception (C_r of 2.65) as the separation value. The area of overlap by the Gaussian curves (46.20 per cent), which is the region where classifications are ambiguous is taken as the sample classification contamination. Three galaxies with very high concentration index (C_r) values of greater than 4 were considered outliers in the Gaussian fitting, and not included in the classification. The singly isolated sample classified is comprised of 3699 galaxies. The galaxies with $C_r \leq 2.65$ represent the late type (mostly spirals), while C_r of greater than 2.65 classified as early type (mostly ellipticals). From the sample, 1856 galaxies (50.18 per cent) were late types, while 1843 (49.82 per cent) classified as early types. A comparison of this results with the visual classifications from the Galaxy Zoo catalogue is presented in the next section. Table 1 provides a summary of the results.

3.1.2 Visual morphology and comparison with concentration index

We obtained visual classifications from the Galaxy Zoo and divided our isolated sample into spiral and elliptical categories. With spectroscopically observed 3537 galaxies from our isolated galaxy sample, we visually classified 3528 galaxies, 2414 (68.42 per cent) as isolated spirals and 1114 (31.58 per cent) isolated ellipticals as shown in Table 2. Nine galaxies had a tie in their classification (p_el_debiased = p_cs_debiased) and considered uncertain.

In comparing the visual classifications with automated classifications by the concentration index, we define the reliability of the classification as the correctly classified fraction of galaxies from the selected subsample. The completeness is defined as a fraction of a given type of galaxies selected by the classification scheme. The contamination is the fraction of misclassified galaxies selected by the classification scheme. This is as illustrated by Strateva et al. (2001).

The concentration index reliably classified 1746 of the 3528 isolated galaxies as late types and 1782 as early types with 1636 of the late-type galaxies being visually spirals and 1004 of the early types being visually ellipticals. The reliability of the concentration index classification for selecting isolated spiral galaxies is 93.70 per cent and 56.34 per cent for selecting isolated elliptical galaxies. The concentration index classified 1636 out of 2414 isolated spiral galaxies as late type and selected 1004 out of the 1114 isolated elliptical galaxies as early type. This results in a completeness of 67.77 per cent for the selected isolated spirals and 90.12 per cent for selected isolated ellipticals. The late-type galaxies have a contamination of 6.30 per cent, while the early-type galaxies have a contamination of 43.66 per cent. The classification comparison results are shown in Table 3.

With the concentration index classifier, our isolated sample selected as early type is highly contaminated and less reliable. Equally, the fraction of isolated spiral galaxies selected as late type is relatively less complete. However, a good enough fraction of 3258 (95 per cent) out of our sample of 3702 isolated galaxies have visual morphologies available in the Galaxy Zoo project. For this reason, we adopted the visual morphological classifications in the follow-up analysis.

For the Coma cluster galaxies, 590 out of the 850 galaxies were spectroscopically observed. 586 coma galaxies were classified into their respective morphologies, 372(63.48 per cent) coma ellipticals and 214(36.52 per cent) coma spirals, with the other four galaxies having a tie, hence considered uncertain. This visually classified Coma cluster sample is used through out our analysis. The visual morphological classifications are also tabulated in Table 2.

3.2 Colour, magnitude, and stellar mass estimates

For the analysis of colour and luminosity correlation with morphology, we used a colour–magnitude diagram (CMD), which is a plot of colour against absolute magnitudes. We obtained the colour measurements with the extinction corrected modelMag (dered parameter in casjobs) from the SDSS data base. The magnitude definition is the better of the exponential and de Vaucouleurs profile magnitude fits. We obtained the *r*-band absolute magnitudes following equation

Table 2. The results of the visual classifications from the Galaxy Zoo.

	Spiral	Elliptical	Sum
Coma visual	214(36.52 per cent)	372(63.48 per cent)	586
Isolated visual	2414(68.42 per cent)	1114(31.58 per cent)	3528

(1) from Baldry et al. (2004), where m_r is the extinction corrected modelMag, D_L is the luminosity distance in parsec (pc), and k_r is the k-correction to $z = 0$ (kcorrR parameter) available in the data base. The k-correction values are as described in Beck et al. (2016).

$$M_r = m_r - k_r - 5 \times \log_{10}(D_L/10). \quad (1)$$

The absolute magnitudes in the r band were transformed to R-band magnitudes using equation (2), where M_r is absolute magnitude. For the SDSS colour to B–R colour transformation, we used equation (3) from Niemi et al. (2010).

$$M_R = M_r - 0.35, \quad (2)$$

$$B - R = (g - i) + 0.44. \quad (3)$$

To estimate the stellar masses, M_*, we used the relation by Bell et al. (2003a) for the ratio of stellar mass and light given by equation (4):

$$\log(M_*/h^{-2}M_\odot) = 0.306 + 1.097[g_{\rm petro} - r_{\rm petro}] - 0.1 - 0.4(M_{r-{\rm petro}} - 5\log_{10}(h) - 4.64). \quad (4)$$

We applied extinction corrections with values from SDSS [computed following Schlegel, Finkbeiner & Davis (1998) and Schlafly & Finkbeiner (2010)] and k corrected to $z = 0$, the Petrosian magnitude colour $g_{\rm petro} - r_{\rm petro}$ (in Casjobs, petroMag parameter), which are measured within a circular aperture determined by the shape of the light profile. We also extinction and k corrected to $z = 0$, the r Petrosian absolute magnitude $M_{r\,-\,{\rm petro}} - 5\log(h)$ with values form the SDSS data base. An extra correction of -0.1 mag was applied to the magnitudes of the elliptical galaxy sample, as a result of the total flux being underestimated by the petrosian magnitudes for those galaxies (Bell et al. 2003a; McIntosh et al. 2014; Lacerna et al. 2016).

We separated the red and blue elliptical galaxies in the colour–mass plot, using the relation by Lacerna et al. (2014) in equation (5). The colour is given by $(g - i)$ and $\log(M_*)$ is the log of stellar mass:

$$(g - i) = 0.16(\log M_* - 10) + 1.05. \quad (5)$$

3.2.1 *The isolated galaxies*

For the isolated galaxies colour and magnitude analysis, we found two galaxies ($\alpha_2000 = 209.8012$, $\delta_2000 = 34.29329$, $z = 0.04946$ and $\alpha_2000 = 221.1527$, $\delta_2000 = 16.52559$, $z = 0.02187$) having very high $g - i$ colour of 7.48 and 5.76, respectively. Both sources were classified as spiral galaxies. In addition, one galaxy ($\alpha_2000 = 346.7424$, $\delta_2000 = -9.28614$, and $z = 0.02377$) had a very low M_r absolute magnitude of -14.11 and also a spiral galaxy. The three sources were not included in our subsequent analysis, with the utilised sample including 3525 isolated galaxies.

We plotted a graph of $B - R$ colour against the absolute magnitude M_R for the isolated galaxies as shown in Fig. 2. The blue circles represent isolated spiral galaxies, while the red triangles represent the isolated elliptical galaxies. The right panel of the figure shows the distribution of the $B - R$ colour represented by the blue and the red line for the isolated spirals and elliptical galaxies, respectively. The R-band absolute magnitude distributions are on the top panel.

Table 3. The results of the comparison between the zoo visual morphologies and the concentration index classifications for the isolated sample.

	Spiral	Elliptical	Sum	Reliability (per cent)	Contamination (per cent)
Late type	1636	110	1746	93.69	6.30
Early type	778	1004	1782	56.34	43.65
Sum	2414	1114	3528		
Completeness	67.77 per cent	90.12 per cent			

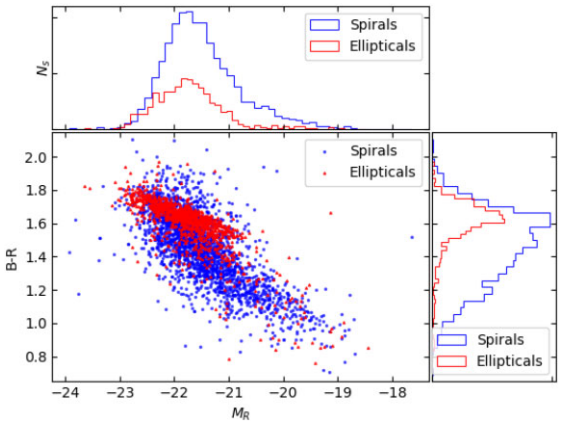

Figure 2. A $B - R$ colour versus M_R absolute magnitude scatter plot and their respective distribution plots for the isolated galaxy sample. The circles and triangles on the scatter plot represent the isolated spiral galaxies and isolated elliptical galaxies respectively. The distribution lines are on the right and top panels .

From Fig. 2, a trend of galaxies becoming redder with increase in luminosity is observed for both the isolated spirals and elliptical galaxies. However, the colour–magnitude relation for the isolated spiral galaxies is steeper than that of their corresponding elliptical sample. Isolated elliptical galaxies are observed to be highly populated on the redder side with a $B - R$ colour of greater than 1.5, while the isolated spirals are extended towards the bluer sides of the diagram. There is still a good number of isolated spiral galaxies at the brighter luminosity and red side of the CMD. The M_R absolute magnitude distributions for the isolated spirals and elliptical galaxies are similar, with the colour overlapping in all magnitude intervals. The distribution similarity is also indicated by the statistical values in Table 4 with both magnitude distributions peaking at almost the same magnitude value.

Fig. 3 shows a graph of colour versus the estimated stellar mass for the isolated galaxy sample. We plotted the $g - i$ colour versus the $\log_{10}$ of stellar mass $M_*/h^{-2}{\rm M}_\odot$. The blue circles represent isolated spirals and the red triangles the isolated ellipticals. The right panel of the figure shows the $g - i$ colour distributions. The blue and red lines represent the isolated spirals and elliptical galaxies respectively. The log stellar mass $M_*/h^{-2}{\rm M}_\odot$ distributions are on the top panel.

For the colour and mass relation, the galaxy colour becomes red with increase in mass. This relation is observed for both the isolated spirals and elliptical galaxies. The isolated ellipticals highly populate the redder and high-mass side of the diagram with a large fraction having stellar masses greater than $10^{10}\,h^{-2}{\rm M}_\odot$. Most of the isolated spiral galaxies have masses below $10^{10.5}\,h^{-2}{\rm M}_\odot$ and their colour extends to the blue side of the diagram. The population of the isolated spiral galaxies seem to be biased towards low masses and bluer colours. Generally, our isolated galaxies have stellar masses below $10^{11.5}$ solar masses.

The isolated spiral galaxies have a mean and median $B - R$ colour of 1.45 and 1.48, and -21.49 and -21.60 M_R absolute magnitude mean and median values, respectively. For the isolated elliptical galaxies, the mean and median $B - R$ colour is 1.59 and 1.62, while

Table 4. The statistical values for colour, absolute magnitude, and stellar mass analysis.

Properties	Spiral galaxies					Elliptical galaxies				
	Mean	σ	0.25	Median	0.75	Mean	σ	0.25	Median	0.75
Isolated galaxy sample										
$B-R$	1.45	0.21	1.30	1.48	1.61	1.59	0.16	1.54	1.62	1.68
M_R	−21.49	0.71	−21.97	−21.601	−21.13	−21.73	0.65	−22.15	−21.77	21.41
$g-i$	1.01	0.21	0.86	1.04	1.17	1.15	0.16	1.10	1.18	1.24
$\log_{10}$ stellar mass	10.21	0.37	10.01	10.27	10.47	10.44	0.32	10.30	10.48	10.65
Coma galaxy sample										
$B-R$	1.36	0.23	1.27	1.42	1.50	1.50	0.13	1.45	1.51	1.59
M_R	−20.57	1.01	−21.25	−20.57	−20.02	−21.09	0.76	−21.60	−21.12	−20.57
$g-i$	0.92	0.23	0.83	0.98	1.06	1.06	0.13	1.01	1.07	1.15
$\log_{10}$ stellar mass	9.85	0.51	9.60	9.91	10.14	10.17	0.37	9.93	10.16	10.40

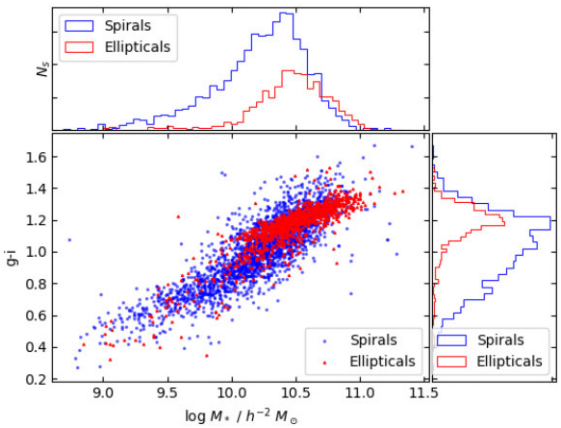

Figure 3. A $g-i$ colour versus the log of stellar mass M_* scatter plot and the respective distribution plots for the isolated galaxies. The circles and triangles with their correspond distribution lines represent the isolated spirals and elliptical galaxies, respectively.

having a mean M_R absolute magnitude of −21.73 and a median magnitude of −21.77. Considering $g-i$ colour, the mean and median values are 1.01 and 1.04 for the isolated spiral galaxies with a mean stellar mass of $10^{10.21}\,h^{-2}\mathrm{M}_\odot$ and a median stellar mass of $10^{10.27}\,h^{-2}\mathrm{M}_\odot$. For the isolated elliptical galaxies, the mean $g-i$ colour is 1.15 and the median colour is 1.18, while having a mean stellar mass of $10^{10.44}\,h^{-2}\mathrm{M}_\odot$ and a median mass of $10^{10.48}\,h^{-2}\mathrm{M}_\odot$. Although the mean and median values for the $B-R$ colour of the two distributions are different, the M_R median values are similar. Nevertheless, the mean and median values for the $g-i$ colour and the stellar mass for the distributions are different. In Table 4, we provide the means, standard deviations, medians, and quartile values at 25 per cent and 75 per cent for our isolated spirals and elliptical galaxies.

3.2.2 *Comparison with the Coma cluster*

In Fig. 4(a), the $B-R$ versus M_R graph for both the coma and isolated elliptical galaxies is shown. The red triangles represent the isolated elliptical sample, while the black squares represent the coma elliptical galaxies. The sample distributions are represented by the red and black lines, respectively. The open magenta squares represent a fraction of the RQEs discussed later in this work. From the graph of $g-i$ colour against log of stellar mass, $M_*/h^{-2}\mathrm{M}_\odot$, for the elliptical galaxies on Fig. 5(a), the red triangles, black squares, and open magenta squares plots with their distributions represent the

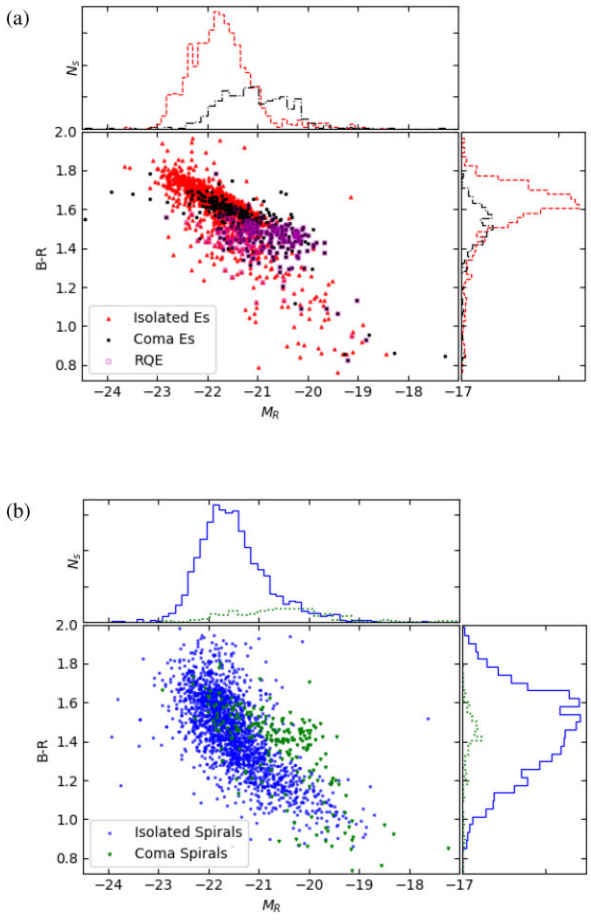

Figure 4. The $B-R$ colour and absolute magnitude M_R relation for the elliptical and spiral samples with the Coma cluster galaxies. Part (a) shows the isolated elliptical galaxies represented by the triangles and the squares representing the coma elliptical galaxies. The circles and inverted triangles in (b) are the isolated and coma spiral galaxies, respectively. The distribution plots are on the top and right panels on both diagrams for the corresponding galaxy samples.

isolated ellipticals, coma ellipticals, and the fraction of the RQEs, respectively. The black solid line is a relation by Lacerna et al. (2014) and is designed to separate red and blue elliptical galaxies.

Observing from Figs 4(a) and 5(a), most of the elliptical galaxies have higher luminosities, larger masses and their correlation with colour is tight. However, our isolated ellipticals colour–magnitude

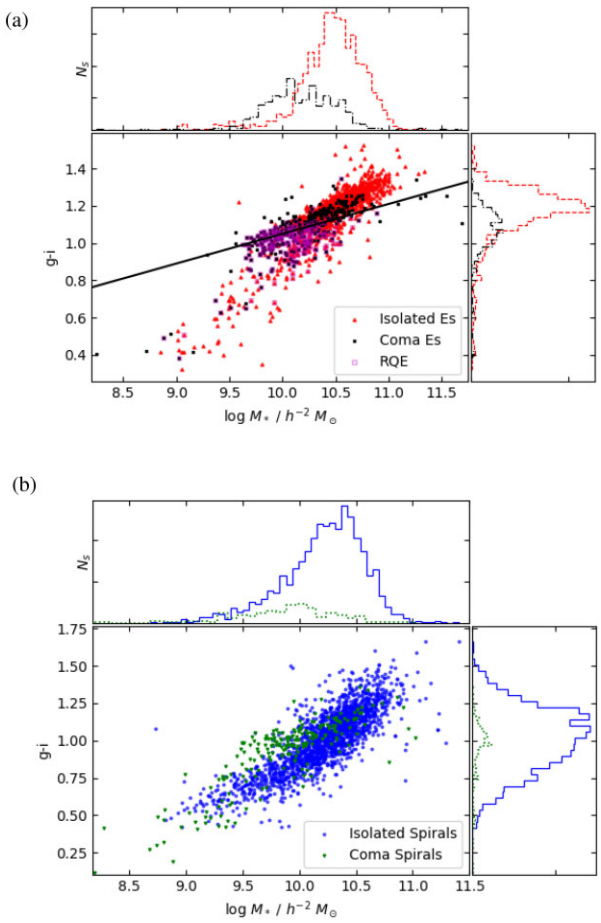

Figure 5. A $g - i$ colour verse the log of stellar mass M_* scatter plot and the respective distribution plots with the coma galaxy sample. In (a), the isolated elliptical and coma elliptical galaxies are represented by the triangles and the squares, respectively. The solid line is from Lacerna et al. (2014) to separate red and blue elliptical galaxies. (b) are the isolated and coma spiral galaxies represented by the circles and inverted triangles. The distribution plots in both diagrams represent the corresponding galaxy samples.

relation is steeper and the galaxies have relatively higher luminosities and redder colour than their corresponding coma elliptical galaxies. This relation is also mirrored in the colour–mass where our isolated elliptical galaxies have a steeper colour relation with stellar mass and averagely massive. Nevertheless, the most luminous and massive elliptical galaxies are found in the Coma cluster sample. As the luminosity becomes fainter and at lower masses, the galaxy population scatters, and the correlation with colour becomes more steep. The scattered population gradually deviates from the red sequence (Figs 4a and 5a, respectively). A good fraction of the ditched population have a $B - R$ colour lesser than 1.4.

Separating the red and blue galaxies with the solid line in Fig. 5(a), it can be seen that most of the elliptical galaxies are red, with a number of galaxies observed to have bluer colours. About 259 (23 per cent) out of 1114 isolated elliptical galaxies are below the line and considered blue in colour. For the Coma cluster about 165 (44 per cent) galaxies out of the 372 coma ellipticals are blue in colour. Elliptical galaxies with blue colour, become bluer with decrease in mass with most of the massive elliptical galaxies being red.

In both Figs 4(b) and 5(b), the blue circles are the isolated spiral galaxies while the green inverted triangles are the coma spiral galaxies. Their distributions are represented by the blue and green lines, respectively. From the two diagrams, the colour–luminosity and colour–mass relations for the isolated spiral galaxies are relatively steeper at higher luminosity and for galaxies with larger stellar masses. Looking at the peak of the galaxy distributions, the isolated spirals are more luminous and massive than their corresponding coma spiral galaxies. A good fraction of red isolated spirals is also observed.

The mean and median $B - R$ colours for the coma elliptical galaxies are 1.50 and 1.51, for the coma spirals 1.36 and 1.42, varying with a standard deviation of 0.13 and 0.23, respectively. The mean and median M_R values are −21.09 and −21.12 for the coma ellipticals, −21.49 and −21.60 for the coma spiral galaxies. For the $g - i$ colour, coma ellipticals have a mean value of 1.06 and a median value 1.07. The coma spirals mean and median, $g - i$ colour values are 0.92 and 0.98, respectively. Stellar mass distribution mean and median statistics for the coma elliptical and spiral galaxies are 10.17, 10.16, and 9.85, 9.91 respectively. The distributions of coma elliptical and spiral galaxies are not similar. These distributions are also significantly different from their respective isolated galaxy sample. See the tabulated results in Table 4.

3.3 Colour–colour selection

Holden et al. (2012) defined a diagonal boundary in the $(u - r)$ and $(r - z)$ colour diagram, that separates passive non-star-forming galaxies without detectable Hα emission, referred to as quiescent galaxies from the star-forming Hα emitters. McIntosh et al. (2014) modified the non-star-forming region by extending the Holden et al. (2012) boundary down to a bluer $(u - r)$ colour, and introduced a criterion to select a fraction of recently quenched galaxies.

To investigate the non-star-forming nature of our galaxy sample and the fraction of recently quenched galaxies, we analysed the galaxies location in the $(u - r)$ versus $(r - z)$ colour space. For the colour, we used the SDSS model magnitudes (model mag) corrected for galactic extinction (dered parameter) and k-corrected to $z = 0$ with corrections from the SDSS data base. We converted the colours to AB system. The SDSS magnitudes on the AB system are such that $m\mathrm{AB} = m + \Delta m$, where Δm equals −0.036, + 0.012, + 0.010, + 0.028, and + 0.040 for u, g, r, i, and z, respectively (Yang et al. 2007).

In our analysis, we separated optimal colour–colour with the selection criterion described by $(u - r) > 2.26$, $(r - z) < 0.75$, and $(u - r) > 0.76 + 2.5(r - z)$ form Holden et al. (2012) with the extension $(u - r) = 1.9$ by McIntosh et al. (2014), to separate the quiescent from the star-forming region. For the recently quenched fraction, we used the criterion introduced by McIntosh et al. (2014) where an extended line $(u - r) > 0.76 + 2.5(r - z)$ from Holden et al. (2012) above, and an added line perpendicular to it with the relation $u - r = 3.67–2.5(r - z)$ was used to identify a sample of RQEs.

3.3.1 The isolated galaxies

In the colour analysis, we plotted the $u - r$ colour versus the $r - z$ colour, extinction, and k-corrected to $z = 0$ and in AB system for the entire isolated galaxy sample. This plot is shown in Fig. 6, where, the isolated spirals and ellipticals representation corresponds with previous diagrams. For the polygon separating quiescent galaxies from star forming, the dotted line is the relation, $u - r = 2.26$ by Holden et al. (2012), and the solid line below it is the extension u

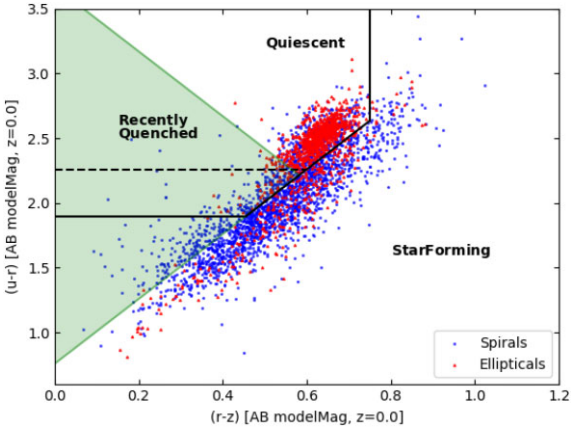

Figure 6. A $(u - r)$ verse $(r - z)$ colour diagram for the isolated sample. The circles represent isolated spiral galaxies with the triangles representing the isolated elliptical galaxies. The polygon with the dotted line separating the quiescent and star-forming regions is a relation by Holden et al. (2012) and the solid line below it is McIntosh et al. (2014) extension.

Table 5. The results of Holden et al. (2012) quiescent galaxies selection criterion for the isolated galaxy sample.

	Isolated elliptical	Isolated spirals	Total	Contamination (per cent)
Quiescents	794	493	1287	38.30
Sample	1114	2411	3525	
Percentage	71.27 per cent	20.44 per cent		

$- r = 1.9$ by McIntosh et al. (2014). The green filled triangle is the recently quenched separation described by McIntosh et al. (2014) to distinguish the small fraction of blue RQEs from the whole sample of quiescent elliptical galaxies.

The Holden et al. (2012) boundary distinguishes the quiescent red early-type galaxies (mostly elliptical galaxies) from blue late-type galaxies (mainly spirals) with pure star formation emission well for our isolated sample. From Fig. 6, the isolated elliptical galaxies highly populate the small quiescent region of the colour–colour space with the isolated spirals dominating the extended and fairly narrow star-forming region. With the quiescent galaxies selected by the Holden et al. (2012) boundary expected to be smooth with no spiral arms or dust lines, 794 out of the 1287 isolated galaxies selected are elliptical galaxies and 493 spirals. The quenched red isolated elliptical galaxies selected by this criterion have a contamination of 38.30 per cent from the red isolated spiral galaxies. With the isolated elliptical sample being 71.27 per cent complete, the contaminating fraction is about 20.44 per cent of the total isolated spiral galaxy sample. The results are summarised in Table 5.

3.3.2 Comparison with the Coma cluster

The $u - r$ versus $r - z$ colour diagram for the coma elliptical galaxy comparison is represented in Fig. 7(a). The red triangles are the isolated elliptical galaxies and the black squares represent the coma elliptical galaxies. The polygon separating quiescent from star-forming galaxies with the dotted and solid lines are the separation by Holden et al. (2012) and McIntosh et al. (2014), respectively. The recently quenched separation described by McIntosh et al. (2014) is the triangle filled in green as before. The fraction selected as

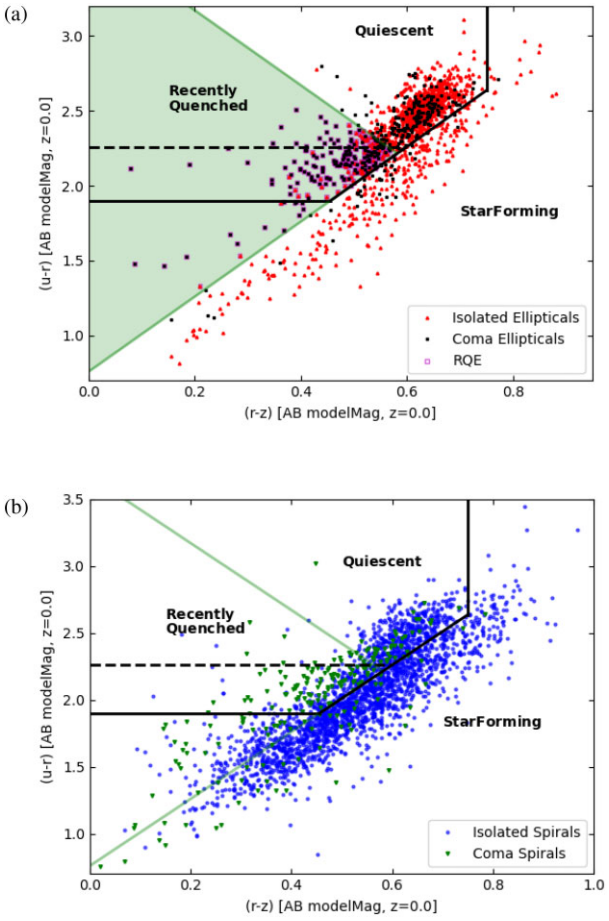

Figure 7. A $(u - r)$ verse $(r - z)$ colour diagram for the comparison with the Coma cluster galaxies. In (a), the triangles and the squares represent the isolated and coma elliptical galaxy samples, respectively. The recently quenched separation by McIntosh et al. (2014) is the filled triangle with the RQEs fitted with the open squares. (b) is the spiral plot representation with the circles and inverted triangles corresponding to isolated and coma spiral galaxies.

the RQEs are fitted with open magenta squares for this and other elliptical galaxies analysis plots.

Following Fig. 7(a), 321 (86.29 per cent) of the 372 coma ellipticals are well selected as quiescent galaxies with McIntosh et al. (2014) extended solid line. 24.32 per cent (271) of our isolated elliptical galaxies are in the star-forming region with only 10.22 per cent (38) of the coma ellipticals selected as star forming. With most elliptical galaxies dominating the quiescent region, there is an observed good fraction of isolated ellipticals in the star-forming region extending towards bluer $u - r$ and $r - z$ colours, and very few star-forming coma elliptical galaxies closer to the separation line.

According to McIntosh et al. (2014), the RQEs are mainly blue, with less than 3 Gyr light-weighted stellar ages, and lack detectable emission responsible for star formation. The star formation histories for the RQEs are different from equally young and blue early-type galaxies that are star forming. Considering their solar metallicities, they 'are consistent with chemical enrichment from a significant merger-triggered star formation event' before the quenching. The authors conclude that RQEs are likely 'first generation' elliptical galaxies formed in a relatively recent major spiral-spiral merger.

In our analysis, 62 isolated elliptical galaxies (5.56 per cent) and 165 (44.35 per cent) coma ellipticals are classified as RQEs following

the criterion by McIntosh et al. (2014, represented as the green filled triangles in Figs 6 and 7a). The fraction of RQEs is larger in our coma sample. About 90.32 per cent (56) of the recently quenched isolated ellipticals and 117(90.91 per cent) in the coma are blue based on the separation in Fig. 5. Our red RQEs in both the isolated and Coma cluster are among the low-mass red elliptical galaxies. On average, the RQEs have moderate stellar masses with none having masses larger than $10^{11}\,h^{-2}\mathrm{M}_{\odot}$. Most of our RQEs have stellar masses between 10^{10} and $10^{10.5}$ solar masses. However, a significant fraction of the recently quenched coma ellipticals have masses lower than $10^{\,10}\,h^{-2}\mathrm{M}_{\odot}$.

As in Fig. 7(b), blue circles are the isolated spirals and the green inverted triangles are the coma spiral galaxies. From the diagram, a linear and tighter $r-z$ and $u-r$ colour–colour correlation is seen in the distribution of our spiral galaxies. The coma spiral galaxies are mostly within the quenched boundary while a higher percentage of our isolated spirals are following the extended star-forming region. An observed fraction of red isolated spirals in the quiescent region of the diagram highly contaminates the early-type galaxies selected with the colour–colour criterion.

3.4 Star formation rates

In estimating the SFRs from Hα luminosity, we adopted the Kennicutt calibration (Kennicutt 1998), assuming a Salpeter initial mass function (IMF) and a mass range from 0.1 to 100 $\mathrm{M}_{\odot}$, given in equation (6).

$$\mathrm{SFR}_{\mathrm{H}\alpha}(\mathrm{M}_{\odot}\mathrm{yr}^{-1}) = 1.27\times10^{-34}L_{\mathrm{H}\alpha}, \tag{6}$$

$L_{\mathrm{H}\alpha}$ is given by equation (7), while $M_{\odot}$ is the mass of the Sun (Hopkins et al. 2001, 2003),

$$L_{\mathrm{H}\alpha}(W) = 4\pi\, D_L^2 (F_{\mathrm{H}\alpha}/10^7) 10^{-0.4(r\mathrm{petro}-r\mathrm{fibre})}\,\frac{(F_{\mathrm{H}\alpha}/F_{\mathrm{H}\beta})}{2.86}^{2.114}. \tag{7}$$

The total galaxy flux is represented by the petrosian magnitude r_{petro}, r_{fibre} is the r fibre magnitude given as an output of the photometric pipeline corresponding to the magnitude through the fibre of 3 arcsec diameter, $F_{H\alpha}$ and $F_{\mathrm{H}\beta}$ are the Hα and Hβ emission fluxes respectively, while D_L^2 is the luminosity distance. The specific star formation rate (sSFR) is defined as the star formation rate per unit stellar mass.

3.4.1 The isolated galaxies

For the SFR estimates, out of the 3525 isolated galaxies used in previous analysis, only 3509 galaxies had the required information for the estimation of the SFRs. We selected the galaxies with Hα and Hβ emission fluxes greater then zero for which we could estimate their SFRs. The fraction with our flux requirement included only 3430 isolated galaxies, with 2379 isolated spirals and 1051 isolated ellipticals. This is the sample we used in this analysis.

A plot of the sSFRs versus the galaxies stellar masses for the isolated galaxies is shown in Fig. 8. The isolated spiral galaxies are represented by the blue circles and the red triangles represent the isolated elliptical galaxies. On the right panel, the distributions of the sSFRs for the isolated spirals and elliptical galaxies are represented by blue and red lines respectively.

The distribution of sSFRs depend on stellar masses. As can be observed in Fig. 8, the sSFRs, generally decrease at larger stellar masses with the dependency on mass being slightly less at lower stellar masses ($<10^{\,10}\,h^{-2}\mathrm{M}_{\odot}$). At masses greater than $10^{\,10}\,h^{-2}\mathrm{M}_{\odot}$, there is an observed sharp decrease in the sSFRs for both the isolated

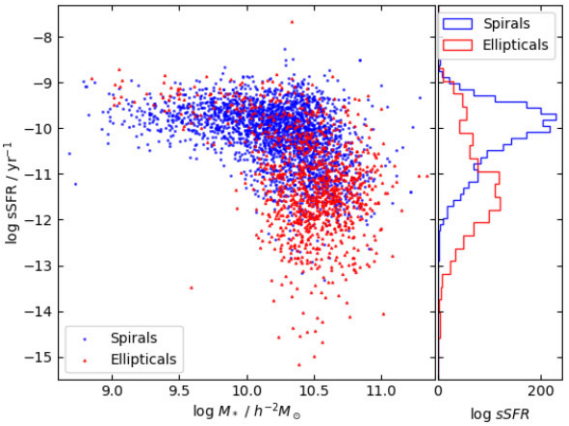

Figure 8. The sSFR versus galaxies stellar mass plot for the isolated sample. The spiral and elliptical galaxies are represented by the circles and the triangles, respectively. Their respective sSFR distributions are on the right panel.

spirals and elliptical galaxies. Generally, there is a mass dependence on the isolated galaxies SFRs, where, lower mass isolated galaxies are in the active star-forming region with higher sSFRs, while the passive region is mainly characterized by massive galaxies. At log sSFR/yr^{-1} of -11, we observe a bimodality in the distribution of our isolated sample. The isolated spiral galaxies populate the active and highly star-forming part of the diagram with higher sSFRs, while the isolated elliptical galaxies show a high preference for occupying the passive region with lower sSFRs.

3.4.2 Comparison with the Coma cluster

From the 586 morphologicaly classified Coma cluster galaxies, only 580 had the required emissions for star formation analysis. Selecting non-zero Hα and Hβ emission fluxes for the SFRs estimation, we utilised a sample of 446 coma galaxies, 291 coma elliptical galaxies, and 155 coma spiral galaxies.

In Fig. 9(a), we plotted the sSFRs diagram for the elliptical galaxies. The isolated elliptical galaxies are plotted as red triangles and the black squares are the coma elliptical galaxies. The fraction of the recently quenched galaxies are fitted with the open magenta squares. We investigated the SFRs for the selected star-forming isolated elliptical galaxies in the colour–colour analysis (Fig. 7), fitted with the open cyan circles. The galaxy distributions are indicated by the respective lines on the right panel.

From Fig. 9(a), a good fraction of the isolated elliptical galaxies occupy the active star formation part that is mostly dominated by the population of the star-forming isolated spiral galaxies (see Fig. 8). This is also indicated by a small peak in the distribution of the isolated ellipticals ($-10 <$ log sSFR/yr^{-1} < -9). The active isolated elliptical galaxies highly correspond to the fraction of star-forming isolated ellipticals selected in the colour–colour diagram, which are indicated by the open cyan circles in the plot, with their distribution mimicking the observed peak (see Fig. 7). The coma elliptical galaxies highly dominate the passive star-forming region. Even the very few selected as star-forming coma ellipticals in the colour–colour analysis are mostly close to the separation line (Fig. 7) and have mainly passive star formation. The recently quenched fraction for both the isolated and coma elliptical galaxies are predominantly in the lower mass passive region with the medium mass occupying the upper part of

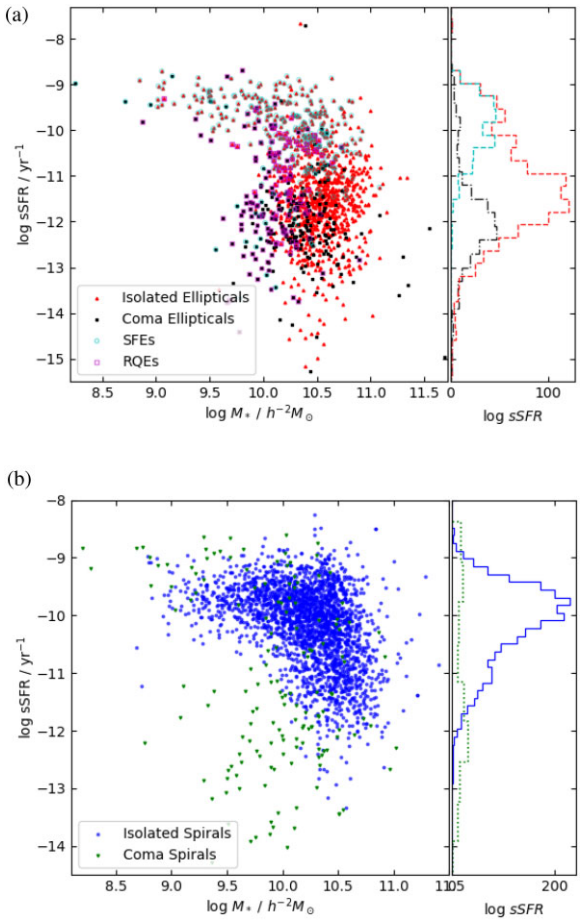

Figure 9. sSFR and stellar mass plot with the Coma cluster galaxies. (a) is the plot for elliptical galaxies. The triangles and squares are the isolated and coma elliptical galaxy samples. The open squares fit the RQEs. The open circles fit the population of star-forming elliptical galaxies selected by the colour–colour analysis. In (b), the circles represent the isolated spirals and inverted triangles correspond to the coma spiral galaxies. The respective distributions are on the side panels.

the passively evolving galaxies. Generally, quiescent galaxies have higher masses and very low sSFRs.

In Fig. 9(b), the blue circles are the isolated spirals and the green inverted triangles are the coma spiral galaxies. The respective distributions are on the side panel. From the plot, although the isolated spiral galaxies are highly in the active star-forming region, there is a small peak at lower sSFRs (about -11 log sSFR/yr^{-1}), with a population of passively evolving isolated spiral galaxies. For the coma spiral galaxies, there is a fraction with very active star formation activities. However, a large enough fraction of the coma spiral galaxies have passive star formation with sSFRs below -11 log sSFR/yr^{-1}.

4 DISCUSSION

4.1 Morphological classification

Using the concentration index (C_r), Shimasaku et al. (2001) pointed out that samples of late and early type galaxies can be automated following the tight correlation with the morphological type. From Fig. 1, the concentration index highly correlates with galaxy morphology, with early-type galaxies having higher concentration index values than the late types, as in Strateva et al. (2001). Following the bimodal distribution in our isolated sample, we separated late- and early-type galaxies by a concentration index of 2.65, with a contamination of 46.20 per cent across the sample.

Comparing the concentration index with the zoo visual classifications, selected isolated spiral galaxies are complete to 67.77 per cent and isolated ellipticals complete to 90.12 per cent. Despite the relative completeness of the selected subsamples, by the concentration index, the isolated early-type galaxies are highly contaminated (43.66 per cent) and less reliable (56.34 per cent), while the isolated late-type galaxies are 93.70 per cent reliable and 6.30 per cent contaminated. Shimasaku et al. (2001) also noted their concentration index selected early-type galaxies (E/S0) being contaminated by spiral galaxies (Sa). McIntosh et al. (2014) pointed out that a crude concentration cut is poor for selecting a pure elliptical galaxy sample from the blue cloud. Our large fraction of isolated spiral galaxies (68.42 per cent) equally contribute to the high contamination percentage on the early type sample. However, with 95 per cent (3528) of our isolated galaxies having visual morphological classifications from the Galaxy Zoo, we adopted the visual classifications in our analysis.

Following the visual classifications, the spiral galaxies dominate the isolated sample by 68.42 per cent with 31.58 per cent elliptical galaxies, while the Coma cluster sample is dominated by 63.48 per cent elliptical galaxies and 36.52 per cent being spiral galaxies. The large fraction of isolated spiral galaxies is supported by observations from Buta et al. (2019) where, their spiral galaxies, constituting nearly 85 per cent of their isolated sample, dominated the morphology. Hernández-Toledo et al. (2010) had a similar observation of the spiral galaxies dominating their isolated sample. This suggests that, the isolated environment does not highly favour the formation of elliptical galaxies.

4.2 Colour, magnitude, and stellar masses

Luminous galaxies are generally well known to be redder in colour than less-luminous galaxies. This supports the observed general trend of galaxies becoming redder with increasing luminosity for both the isolated spirals and isolated elliptical galaxies. With our isolated elliptical galaxies highly populating the redder side, while the isolated spirals extend towards the bluer sides of the CMD, there is an observed significant fraction of relatively luminous and red isolated spiral galaxies. The M_R absolute magnitude distributions for the isolated spirals and elliptical galaxies being similar, with their colour overlapping at practically all absolute magnitude intervals observed in our analysis (as in Fig. 2), was also noted by Hernández-Toledo et al. (2010). As a result of the overlap in colour, the colour index cannot suitably separate the two distributions without a very large contamination for the isolated sample.

Kauffmann et al. (2002), when studying the stellar masses for the whole SDSS parent sample, observed ordinary galaxies dividing into two definite categories at a stellar mass of $3 \times 10^{10} h^{-2}M_\odot$. This distribution of mass is not obvious for our sample of isolated galaxies. However, a large fraction of the isolated elliptical galaxies have stellar masses greater than $10^{10} h^{-2}M_\odot$. This is the cut mass used by McIntosh et al. (2014) to identify a sample of RQEs. Additionally, most of our isolated spiral galaxies have masses below $10^{10.5} h^{-2}M_\odot$. It can be noted that, using a cut in mass to separate the sample of isolated elliptical galaxies requires an additional cleaning method to avoid the extreme contamination by the massive isolated spiral galaxies. In general, our isolated galaxies have relatively lower stellar masses of below $10^{11.5}$ solar masses. This was earlier noted by Hirschmann et al. (2013) when analysing their 3D (no neighbour

within a circular sphere of 1 Mpc) modelled sample. Other studies of isolated galaxies seem to also confirm this observations (Fernández Lorenzo et al. 2013; Lacerna et al. 2016), indicating the isolation criteria used limites the isolated sample to relatively lower mass galaxies.

In comparing colour–maginitude and colour–mass relations with the Coma cluster galaxies, the relations are steeper in our isolated sample. Our isolated ellipticals have steeper colour, magnitude, and mass relations with relatively higher luminosities, redder colour, and averagely massive than their corresponding coma elliptical galaxies. However, the most luminous and massive elliptical galaxies are found in the Coma cluster sample. This indicates that the dense environments are the home of very massive elliptical galaxies. The steepness in colour relation suggest a faster transition to the red sequence for the isolated galaxies. Lacerna et al. (2016) also found a similar fast transition of their isolated ellipticals to the red sequence.

At fainter luminosities and lower stellar masses, there is an observed population of elliptical galaxies, mainly isolated ellipticals, with bluer colours that ditches from the red sequence, in Figs 4(a) and 5(a). This agrees with results from Lacerna et al. (2016), who observed a small fraction of the isolated ellipticals following a different trend, with steeper colour–magnitude relation toward bluer colours as magnitudes became fainter, creating a brunch that gradually deviates from the red sequence. Niemi et al. (2010) also observed a distinct population of their simulated isolated field elliptical galaxies (IfEs) populating the bluer and less-luminous side of the CMD. Most of the galaxies in Niemi et al. (2010) were having $B - R$ colour of less than 1.4 ($B - R < 1.4$), also observed in our Fig. 4(a).

Looking at the red and blue elliptical galaxies separated by Lacerna et al. (2014) criterion in the $g - i$ colour, about 23 per cent of our isolated elliptical galaxies were blue in colour. Our percentage of blue elliptical galaxies is close to that observed by Lacerna et al. (2016) where about 20 per cent of their isolated elliptical galaxies were considered blue with the same criterion. However, our observed fraction of blue elliptical galaxies in the Coma cluster is higher (44 per cent).

The colour–luminosity and colour–mass relations for our isolated spiral galaxies, at higher luminosities and relatively larger stellar masses, are steeper than for their corresponding coma spiral galaxies. Looking at the distribution peaks, isolated spirals are relatively luminous and massive than the coma spiral galaxies. There is also a good fraction of observed red isolated spirals galaxies. Fernández Lorenzo et al. (2013) had observed massive spirals in less dense environment being large in size compared to those in dense environment.

4.3 Colour–colour analysis

The Holden et al. (2012) boundary distinguishes the quiescent early-type galaxies from the blue late-type galaxies well for our isolated sample. The isolated elliptical galaxies occupy a small quiescent region, with isolated spirals dominating the extended star-forming region. This supports the well-known notion that most elliptical galaxies are older and have quenched their star formation, while the spiral galaxies are younger and star forming.

Holden et al. (2012) found about 82 per cent of their early-type quiescent galaxies within the boundary, with a contamination of 18 per cent star-forming late types. In our isolated galaxies, 71.27 per cent of the elliptical galaxies were selected within the boundary, having a 38 per cent contamination fraction from red spirals. The large contamination of the quenched red isolated ellipticals with the red isolated spirals can be attributed to the general large number of spiral galaxies, and a good fraction of red spirals in our sample. The completeness of the selected quiescent isolated ellipticals can be complimented by the significant fraction of isolated ellipticals in the star-forming region. Although the $(u - r)$ colour index is greatly effective at distinguishing among the different galaxy types, Hernández-Toledo et al. (2010) also observed a significant overlap of their early- and late-type isolated galaxies distribution at redder colours.

Most of the coma elliptical galaxies (86.29 per cent) are selected as quiescent following McIntosh et al. (2014) extended line. The 24.32 per cent fraction of isolated elliptical galaxies in the star-forming region, extending towards bluer $u - r$ and $r - z$ colours, corresponds to the ditched population of isolated ellipticals in our colour–magnitude and colour–mass analysis (see Figs 4 and 5, respectively). With the significant fraction of star-forming isolated elliptical galaxies, the fraction of coma ellipticals in the star-forming region is relatively small (10.22 per cent), and mostly closer to the separation line. From a similar colour–colour diagram in Lacerna et al. (2016, their fig. 5), some of their isolated elliptical galaxies extended towards the star-forming region, while their coma ellipticals were within the non-star-forming region or close to the separation line.

5.56 per cent of our isolated elliptical galaxies and 44.35 per cent of the coma ellipticals are RQEs with McIntosh et al. (2014) criterion. Lacerna et al. (2016) observed about 10 per cent (9) of their isolated elliptical galaxies being RQEs according to this criterion and one RQE candidate in their coma supercluster sample closer to the lower boundary. Their analysis was done on elliptical galaxies with masses greater than $10^{10}\,h^{-2}\mathrm{M}_{\odot}$. However, the fraction of RQEs observed in our Coma cluster sample have stellar masses lower than $10^{10}\,h^{-2}\mathrm{M}_{\odot}$. Most of the recently RQEs have moderate stellar masses with none having a mass lager than $10^{11}\,h^{-2}\mathrm{M}_{\odot}$. For the isolated ellipticals, the recently quenched fraction has mainly masses above 10^{10} and within an upper bracket of $10^{10.5}$ solar masses. Most of the RQEs in McIntosh et al. (2014) also have stellar masses below 10^{11} solar masses. The observation of RQEs having moderate mass both in the isolated and coma samples, supports the idea that most quiescent galaxies are massive and form through accumulation of mass.

90.32 per cent and 90.91 per cent of our recently quenched isolated and coma ellipticals are blue based on the separation in Fig. 5. Our red recently quenched population is among the lower mass red elliptical galaxies in both samples, respectively. Lacerna et al. (2016) found seven out of nine of their RQEs being blue and the rest red using the same colour separation. This supports the analysis by McIntosh et al. (2014) that most of the RQEs are blue. To confirm most massive elliptical galaxies quenched their star formation long ago, our red RQEs are among the 20 per cent low-mass red ellipicals.

A tighter $r - z$ and $u - r$ colour–colour correlation is seen in the distribution of our spiral galaxies. A similar tighter distribution was observed by Hernández-Toledo et al. (2010) in their various colour–colour diagrams for their isolated galaxies. The coma spirals are mostly in the quiescent region following the extended McIntosh et al. (2014) criterion, while a good percentage of our isolated spirals are following the extended star-forming region. The relatively considerable fraction of red isolated spiral galaxies in the quiescent region of the colour–colour diagram suggests a quenched population of spiral galaxies even in our isolated sample. This red isolated spiral fraction also highly contaminates the quiescent isolated early-type galaxies selected with the colour–colour method.

4.4 Star formation rates

Bauer et al. (2013) observed a dependency of sSFRs with stellar mass, for galaxies with redshifts of $z < 0.32$, in the Galaxy And Mass

Assembly survey. The sSFRs decrease with an increase in stellar mass, with a rapid decline at larger stellar masses. In our sample of isolated galaxies, we observed a similar dependency of sSFRs distribution with stellar mass. The sSFRs, in the isolated sample generally decreases at larger stellar masses, with the dependency on mass being slightly less at lower stellar masses ($<10^{10}\,h^{-2}\mathrm{M}_{\odot}$). At masses greater than $10^{10}\,h^{-2}\mathrm{M}_{\odot}$, a sharp decrease in the sSFRs is observed for both the isolated spirals and elliptical galaxies. Generally, the lower mass isolated galaxies occupy the active star-forming region with higher sSFRs, while the passive region is mainly characterized by massive galaxies.

A bimodality in the distribution of our isolated sample is observed, where the isolated spiral galaxies have higher sSFRs and populate the active and highly star-forming part of the diagram. The isolated elliptical galaxies strongly occupy the passive region where the sSFRs are lower. This bimodality in the sSFRs distribution was also observed by Hirschmann et al. (2013), in the study of their isolated model galaxies. For the isolated galaxies, the two distributions can be separated by a cut at log sSFR/yr^{-1} of -11 which correspond to the intercept of the isolated spiral and elliptical distributions.

With the isolated elliptical galaxies highly occupying the passive region, a good fraction is observed to occupy the active star-forming region dominated by star-forming isolated spiral galaxies shown in Fig. 8. This is also supported by the small peak observed in the distribution. However, the coma elliptical galaxies dominate the passive region. Lacerna et al. (2016) found nearly all their coma ellipticals passive with only one in the star-forming region. They did not observe a difference in the distributions. However, they noted a small fraction of their isolated ellipticals at stellar masses $< 10^{10.7}\,h^{-2}\mathrm{M}_{\odot}$, with relevant signs of star formation. The fraction of active star-forming isolated ellipticals highly correspond to the star-forming isolated ellipticals selected in the colour–colour diagram. This agrees with Lacerna et al. (2016) observations of an agreement between the isolated elliptical galaxies identified as star-forming in their colour—colour selection and the actively star-forming isolated ellipticals in their sSFR diagram (figs 3 and 5 in Lacerna et al. 2016). The few coma ellipticals in the star-forming region of the colour–colour analysis (see Fig. 7) are mostly close to the separation line and have mainly passive star formation.

The recently quenched fraction of both the isolated and coma elliptical galaxies highly populate the lower mass passive region with the medium mass occupying the upper part of the passively evolving galaxies. The quiescents have higher masses and very low sSFRs supporting the idea that they are old and dead with no active star formation. Lacerna et al. (2016) had eight out of their nine RQEs in the passive region and the only one actively blue star forming had active galactic nucleus emission.

While the isolated spiral galaxies are mainly in the active star-forming region, the small peak in the distribution at lower sSFRs suggest a fraction of passively evolved high-mass spiral galaxies in the isolated sample. For the coma spirals, although there is a fraction with very active star formation activities, a larger fraction of the coma spiral galaxies have passive star formation activities, with sSFRs below -11 log sSFR/yr^{-1}. Hirschmann et al. (2013) in their analysis found the isolated galaxies having a high percentage of star-forming galaxies than their mass-matched random sample (with log sSFR/yr$^{-1} > -11$). This could suggest the environmental contribution on the star formation activities in galaxies, where there is supration of star formation in the dense environment, even for spiral galaxies.

5 CONCLUSIONS

To understand our isolated galaxy sample consisting of 3702 single isolated galaxies, a morphological classification into early type (with mostly ellipticals) and late type (mainly spirals) was required. Two methods were considered; the central concentration index tool and the visual classification method. Although the visual inspection method is known to be time consuming and labour intensive, we used already existing visual classifications by the Galaxy Zoo project obtained from the SDSS archive. The isolated sample was initially classified using the concentration index, C_r value of 2.65, obtained following the bimodal distribution of the sample. 49.82 per cent and 50.18 per cent of the isolated sample was classified as early and late types, respectively, with 46.20 per cent contamination across the sample. Comparing the concentration index and visual classifications, the isolated spiral galaxies selected by the concentration index are 67.77 per cent complete and the selected isolated ellipticals are 90.12 per cent complete. However, the reliability of the late-type sample is 93.69 per cent and the early-type galaxies are 56.34 per cent reliable with a significant contamination by the isolated spiral galaxies (43.65 per cent contamination). Despite early-type galaxies being contaminated by spiral galaxies in concentration index selected samples, the higher contamination percentage in our isolated sample can be attributed to the large fraction of the isolated spiral galaxies. With the visual classifications, our isolated galaxy sample is highly dominated by 68.42 per cent spiral galaxies, while the coma sample is dominated by 63.48 per cent elliptical galaxies.

In the analysis of colour, magnitude, and stellar mass relations, the isolated elliptical galaxies are mainly characterized by redder, massive and more luminous galaxies. The isolated spiral galaxies seem to be biased towards being blue, less-massive, and less-luminous. However, a significantly larger fraction of isolated red spiral galaxies with larger stellar masses and high luminosities was observed. Using a cut in mass to separate the sample of isolated elliptical galaxies requires an additional cleaning method to avoid the extreme contamination by the massive isolated spiral galaxies. In both the colour–magnitude and colour–mass analysis, the isolated spiral galaxy relations are steeper than the isolated elliptical galaxies, which have a less steep but tight correlation with colour. However, both the isolated spirals and ellipticals have steeper colour relations than their corresponding coma galaxies. This suggest a fast transition to the red sequence for the isolated galaxies. There is an overlap between the isolated spiral and the elliptical galaxies across all absolute magnitude intervals. This overlap suggests that, for the isolated galaxy sample, the colour index is not suitable to effectively separate the two distributions without a large contamination. Our isolated sample is limited to galaxies with masses relatively lower than $10^{11.5}$ solar masses. The most luminous and massive elliptical galaxies are found in the Coma cluster sample. A small fraction of the isolated elliptical galaxies is noted to be following a different trend and mostly dominated by the blue elliptical galaxies. A slightly different distribution of the isolated spiral galaxies characterized by lower stellar mass, blue spirals and having a less steep relation is observed at lower luminosities.

As observed in the colour–colour analysis, the $u - r$ and $r - z$ colours have a general tight correlation with each other. In the colour–colour diagram, the isolated elliptical galaxies are occupying a small region and are well selected as quiescent galaxies as seen in our Fig. 6. The isolated spiral galaxies are strongly following the extended and fairly narrow star-forming region. There is a fraction of isolated elliptical galaxies (24.32 per cent) selected in the star-

forming region, extending towards bluer $u - r$ and $r - z$ colours, which corresponds to the ditched population of isolated ellipticals in our colour–magnitude and colour–mass analysis. Despite the $(u - r)$ colour index being effective at distinguishing among the different galaxy types, the overlap of isolated elliptical and spiral galaxies distribution, at redder colours, contaminate the selected early-type galaxies by 30 per cent with isolated spiral galaxies. The high contamination of the early-type galaxies can be from the general large number of isolated spirals and the reasonable fraction of red isolated spiral galaxies in the sample. Our isolated sample also has a slightly higher percentage of blue elliptical galaxies. A 5 per cent fraction of the isolated elliptical galaxies are noted to be RQEs, having recently quenched their star formation and are transiting to the red sequence. A very large fraction (90 per cent) of the RQEs are blue. The red RQEs are among the 20 per cent low-mass red elliptical galaxies confirming that most massive elliptical galaxies quenched their star formation long ago.

While the distribution of the sSFRs is expected to depend on stellar masses, there is a general decrease of the sSFRs at larger stellar masses for our isolated sample. The dependency of the sSFR on stellar mass is observed to be slightly less at lower masses, and the relation is almost flat with a very sharp decrease at larger stellar masses. Looking at the galaxies distribution of sSFRs, a strong bimodality in the distribution of our isolated galaxies is observed which can be separated by a cut at log sSFR/yr^{-1} of -11. The isolated spiral galaxies have higher sSFRs and populate the active and highly star-forming region, and the isolated elliptical galaxies occupy the passive region and have lower sSFRs. Some notable peaks in the distribution of our isolated galaxies, indicate a fraction of passively evolving high-mass isolated spiral galaxies, and actively star-forming isolated elliptical galaxies that highly correspond to a similar selection in the colour–colour diagram. In general, the low-mass galaxies have higher sSFRs, while the passively evolving galaxies are characterized by massive galaxies. The RQEs with lower masses have passive emissions and those with medium mass occupy the upper part of the passive galaxies. The characteristics of quiescent elliptical galaxies of having high stellar masses and very low sSFRs confirms their old and dead nature.

ACKNOWLEDGEMENTS

Funding for the SDSS-IV has been provided by the Alfred P. Sloan Foundation, the U.S. Department of Energy Office of Science, and the Participating Institutions. The SDSS website is https://www.sdss4.org.

SDSS-IV is managed by the Astrophysical Research Consortium for the Participating Institutions of the SDSS Collaboration including the Brazilian Participation Group, the Carnegie Institution for Science, Carnegie Mellon University, the Chilean Participation Group, the French Participation Group, Harvard-Smithsonian Center for Astrophysics, Instituto de Astrofísica de Canarias, The Johns Hopkins University, Kavli Institute for the Physics and Mathematics of the Universe (IPMU)/University of Tokyo, Korean Participation Group, Lawrence Berkeley National Laboratory, Leibniz Institut für Astrophysik Potsdam (AIP), Max-Planck-Institut für Astronomie (MPIA Heidelberg), Max-Planck-Institut für Astrophysik (MPA Garching), Max-Planck-Institut für Extraterrestrische Physik (MPE), National Astronomical Observatories of China, New Mexico State University, New York University, University of Notre Dame, Observatário Nacional/MCTI, The Ohio State University, Pennsylvania State University, Shanghai Astronomical Observatory, United Kingdom Participation Group, Universidad Nacional Autónoma de México, University of Arizona, University of Colorado Boulder, University of Oxford, University of Portsmouth, University of Utah, University of Virginia, University of Washington, University of Wisconsin, Vanderbilt University, and Yale University.

DATA AVAILABILITY

The data used in this work are publicly available. The catalogue of isolated galaxies can be found on https://cdsarc.cds.unistra.fr/viz-bin/cat/J/A + A/578/A110. The WCS catalogue of the Coma cluster is available though https://cdsarc.cds.unistra.fr/viz-bin/cat/J/A + A/650/A76. The analysis was done using data from SDSS-DR 16, which is accessible through https://www.sdss4.org.

REFERENCES

Ahn C. P. et al., 2014, ApJS, 211, 17
Ahumada R. et al., 2020, ApJS, 249, 3
Argudo-Fernández M. et al., 2015, A&A, 578, A110
Baldry I. K., Glazebrook K., Brinkmann J., Ivezić Ž., Lupton R. H., Nichol R. C., Szalay A. S., 2004, ApJ, 600, 681
Bauer A. E. et al., 2013, MNRAS, 434, 209
Beck R., Dobos L., Budavári T., Szalay A. S., Csabai I., 2016, MNRAS, 460, 1371
Bell E. F., McIntosh D. H., Katz N., Weinberg M. D., 2003a, ApJS, 149, 289
Bell E. F. et al., 2003b, ApJ, 600, L11
Biviano A., Durret F., Gerbal D., LeFevre O., Lobo C., Mazure A., Slezak E., 1995, A&A, 311, 95
Blanton M. R. et al., 2003, ApJ, 592, 819
Bolzonella M. et al., 2010, A&A, 524, A76
Buta R. J. et al., 2019, MNRAS, 488, 2175
Coziol R., Torres-Papaqui J., Plauchu-Frayn I., Islas-Islas J., Ortega-Minakata R., Neri-Larios D., Andernach H., 2011, Rev. Mex. Astron. Astrofís., 47, 361
De Vaucouleurs G., De Vaucouleurs A., Corwin Jr H., Buta R., Paturel G., Fouque P., 1991, Third Reference Catalogue of Bright Galaxies. Volume I: Explanations and References. Springer, New York, p. 2091
Fernández Lorenzo M., Sulentic J., Verdes-Montenegro L., Argudo-Fernández M., 2013, MNRAS, 434, 325
Fukugita M., Ichikawa T., Gunn J. E, Doi M., Shimasaku K., Schneider D. P., 1996, AJ, 111, 1748
Fukugita M. et al., 2007, AJ, 134, 579
Gabor J., Davé R., Finlator K., Oppenheimer B., 2010, MNRAS, 407, 749
Gunn J. E. et al., 1998, AJ, 116, 3040
Healy J. et al., 2021, A&A, 650, A76
Hernández-Toledo H., Vázquez-Mata J., Martínez-Vázquez L., Choi Y.-Y., Park C., 2010, AJ, 139, 2525
Hirschmann M., De Lucia G., Iovino A., Cucciati O., 2013, MNRAS, 433, 1479
Holden B. P., Van der Wel A., Rix H.-W., Franx M., 2012, ApJ, 749, 96
Hopkins A. M., Connolly A., Haarsma D., Cram L., 2001, AJ, 122, 288
Hopkins A. M. et al., 2003, ApJ, 599, 971
Hopkins P. F., Hernquist L., Cox T. J., Robertson B., Springel V., 2006, ApJS, 163, 50
Kauffmann G. et al., 2002, MNRAS, 341, 33
Kennicutt R. C., Jr, 1998, ARA&A, 36, 189
Lacerna I., Rodriguez-Puebla A., Avila-Reese V., Hernandez-Toledo H. M., 2014, ApJ, 788, 29
Lacerna I., Hernández-Toledo H., Avila-Reese V., Abonza-Sane J., Del Olmo A., 2016, A&A, 588, A79
Lintott C. J. et al., 2008, MNRAS, 389, 1179
Lintott C. et al., 2011, MNRAS, 410, 166
McIntosh D. H. et al., 2014, MNRAS, 442, 533
Nakamura O., Fukugita M., Yasuda N., Loveday J., Brinkmann J., Schneider D. P., Shimasaku K., SubbaRao M., 2003, AJ, 125, 1682

Niemi S.-M., Heinämäki P., Nurmi P., Saar E., 2010, MNRAS, 405, 477
Pozzetti L. et al., 2010, A&A, 523, A13
Schlafly E. F., Finkbeiner D. P., 2011, ApJ, 737, 103
Schlegel D. J., Finkbeiner D. P., Davis M., 1998, ApJ, 500, 525
Shimasaku K. et al., 2001, AJ, 122, 1238
Strateva I. et al., 2001, AJ, 122, 1861
Strauss M. A. et al., 2002, AJ, 124, 1810
Van Den Bosch F. C., Aquino D., Yang X., Mo H., Pasquali A., McIntosh D. H., Weinmann S. M., Kang X., 2008, MNRAS, 387, 79
Van Der Wel A., Van Der Marel R. P., 2008, ApJ, 684, 260
Verdes-Montenegro L., Sulentic J., Lisenfeld U., Léon S., Espada D., Garcia E., Sabater J., Verley S., 2005, A&A, 436, 443
Verley S. et al., 2007, A&A, 470, 505
Vollmer B., 2013, Planets, Stars and Stellar Systems, Vol. 6. Springer, Dordrecht, p. 207
Yang X., Mo H., Van den Bosch F. C., Pasquali A., Li C., Barden M., 2007, ApJ, 671, 153

This paper has been typeset from a TEX/LATEX file prepared by the author.